Pt–Re–Ge/Al₂O₃ catalysts for n-octane reforming: Influence of the order of addition of the metal precursors

Luciene S. Carvalho [a,b], Karla C.S. Conceição [a], Vanina A. Mazzieri [c], Patricio Reyes [d], Carlos L. Pieck [c], Maria do Carmo Rangel [a,*]

[a] Grupo de Estudos em Cinética e Catálise GECCAT, Instituto de Química, Universidade Federal da Bahia, Rua Barão de Geremoabo, 147 Campus Universitário de Ondina, 40170-115 Salvador, Bahia, Brazil
[b] Grupo de Pesquisa e Inovação em Química, Instituto Federal de Educação, Ciência e Tecnologia da Bahia, Campus Camaçari, Loteamento Espaço Alpha (BA 522), Bairro Limoeiro, 42802-590 Camaçari, Bahia, Brazil
[c] Instituto de Investigaciones en Catálisis y Petroquímica – INCAPE – (FIQ, UNL-CONICET), Santiago del Estero 2654, 3000 Santa Fe, Argentina
[d] Departamento de Físico Química, Facultad de Ciencias Químicas, Universidad de Concepción, Casilla 160-C, Concepción, Chile

ARTICLE INFO

ABSTRACT

Trimetallic Pt–Re–Ge supported catalysts for naphtha reforming were prepared by successive impregnation of suitable precursors on gamma alumina. The order of addition of these precursors was varied and its influence on the catalytic properties was assessed by means of the model reaction of n-octane reforming. It was found that the order of addition of the metal precursors greatly affects the performance and properties of these systems, which in turn is closely related to the first impregnated metal. When platinum is impregnated before rhenium and germanium the metals are reduced separately resulting in catalysts with high dehydrogenation activity and low hydrogenolysis activity. On the other hand, the impregnation of germanium before the other metals leads to the production of catalysts with low activities for dehydrogenation and high activity for hydrogenolysis, as a consequence of the strong interactions among the metals. By adding rhenium before the other metals, catalysts with intermediate behavior are produced. For all catalysts, platinum interacts more strongly with rhenium than with germanium. The order of addition does not modify the acidic properties of the support but germanium and rhenium seem to change the acidity of the support in the vicinity of the metals, causing differences in the selectivity to aromatic compounds and paraffinic isomers. These features can be used to tailor catalysts with high selectivity for the production of aromatics or isoparaffins, depending on the purpose of the reforming process. The RePtGe catalyst has the highest selectivity to branched isoparaffins and then can be used to produce isoparaffins-rich gasoline while a reformate rich in aromatics can be obtained by using the GeRePt catalyst.

© 2012 Elsevier B.V. All rights reserved.

1. Introduction

Catalytic naphtha reforming is by far the main commercial route for producing aromatics, high value intermediates used in the manufacture of plastics, nylon, rubbers and polyester fibers, among others. This process is also used to convert linear hydrocarbons into branched ones in order to improve the octane number of gasoline. Hydrogen is obtained as a by-product, which is mainly used in hydrotreatment processes such as hydrodesulfuration and hydrodenitrogenation. According to the current environmental laws, the aromatic content in fuels should be even lower than the previous values. The benzene content in American gasolines should be at maximum 0.62 vol.% by 2015, according to the new regulations of the US Environmental Protection Agency (MSAT II). The restrictions for benzene, the major supplier of octane number to gasoline pool, make important its replacement by other compounds of high RON and with no noxious environmental impact, such as branched isoparaffins.

The huge and complex network of chemical reactions occurring in the catalytic reformer is basically made of only two kinds of reactions: acid-catalyzed and metal-catalyzed ones. Therefore, naphtha reforming catalysts must be bifunctional. The metal function is usually supplied by platinum metal particles highly dispersed on a porous carrier, typically chlorided gamma-alumina. Platinum provides the essential sites for hydrogenation and dehydrogenation. The acid function is supplied by the support itself. While gamma-alumina is amphoteric, the addition of chlorine promotes its acidity and gives to the support the ability to catalyze isomerization and cyclization reactions [1].

* Corresponding author. Tel.: +55 71 3283 6867; fax: +55 71 3235 5166.
E-mail address: mcarmov@ufba.br (M.d.C. Rangel).

A second or third element added to the reforming catalyst modifies both the metal and the acid functions but this addition is almost exclusively intended for fine-tuning the metal function properties. Rhenium, tin, tungsten, iridium, indium and germanium are usually used as additives, producing bimetallic [2–9] or trimetallic catalysts [10–16]. These catalysts show better performances than monometallic platinum catalysts, they are more selective and more resistant against deactivation [2–14,16–20]. The improvement of activity and selectivity of multimetallic systems is attributed to electronic and geometric effects exerted by the other added metals [10,13,21]. Besides, some elements as tin and germanium also modify the acid sites of the support making them more adequate to catalyze the isomerization and cyclization reactions [11,12,21,22]. Furthermore, when rhenium and iridium are added they can get alloyed to platinum thus increasing its activity for hydrogenolysis. This is an undesirable effect because it leads to the formation of light gases, especially methane. In order to reduce the quantity of active sites for this reaction, it is necessary to add sulfur to the metal phase, by sulfidation [11,16]. In this case, the role of sulfur is to diminish the number of sites close to platinum, active for hydrogenolysis. However, so that its effect can be beneficial, the amount of sulfur added should be very small, around one sulfur to four platinum atoms. For higher amounts of sulfur (around one sulfur to two platinum on the surface), sulfur can be irreversibly adsorbed on platinum atoms, completely inhibiting the activity of the metal function of reforming catalysts. The poisoning by sulfur is less for the platinum monometallic catalysts as compared to the multimetallic ones [16].

Nowadays industrial plants of catalytic reforming use state-of-the-art trimetallic catalysts of proprietary composition. It is known, however, that these solids have a formulation of the following type: Pt–Re–M/Al$_2$O$_3$. Many reports have investigated the performance of trimetallic systems such as Pt–Re–Sn [10,12,13] and Pt–Re–Ge/Al$_2$O$_3$ [21,22]. These studies show that the preparation method affects the properties of both the acid and metal functions of the reforming catalyst and consequently its activity, selectivity and resistance against deactivation.

When Pt–Re–Sn/Al$_2$O$_3$ catalysts are prepared by successive impregnation of the metal precursors, the addition of tin before rhenium is more convenient, producing stable catalysts, more active and more selective to the formation of aromatics [10,12]. On the other hand, other works [16,21] have reported that tin and germanium are able to play the role of sulfur in trimetallic catalysts prepared by co-impregnation.

In line with the previous comments, this work is devoted to the study of the performance of Pt–Re–Ge/Al$_2$O$_3$ trimetallic catalysts, prepared by sequential impregnation of the promoters in different orders. n-Octane reforming was used as a model reaction for naphtha reforming. The effect of the order of the metal addition on the properties of the acid and metal functions was also assessed.

2. Experimental

2.1. Catalysts preparation

The support used was a commercial high-purity γ-alumina (Cyanamid Ketjen CK 300). The main impurities were sodium (5 ppm), iron (150 ppm) and sulfur (50 ppm). The extruded alumina pellets were ground and sieved and the 35–80 mesh fraction was separated and calcined under air flow (60 ml min^{-1}) for 3 h, at 650 °C. After calcination, the specific surface area of this support was 180 m^2 g^{-1}, the pore volume was 0.49 cm^3 g^{-1} and the average pore radius was 5.4 nm.

The metals were incorporated by successively impregnating the support with aqueous solutions of their corresponding salts. The amount and concentration of the solutions were adjusted in order to have 0.3% of each metal on the final catalyst. The precursors were H$_2$PtCl$_6$·6H$_2$O (3.345 mg Pt. ml^{-1}), NH$_4$ReO$_4$ (20.18 mg Re. ml^{-1}) and GeCl$_4$ (1.8 mg Ge. ml^{-1}).

Monometallic catalysts: 5 g of Al$_2$O$_3$ were immersed in a 0.2 mol l^{-1} HCl solution (1.5 ml g^{-1}) and then the metal precursor solution was added. After 1 h under stirring, the solvent was slowly evaporated by heating at 70 °C, while stirring gently. The catalyst was then dried at 120 °C overnight, calcined under air flow (60 ml min^{-1}) for 4 h at 500 °C and reduced in hydrogen (60 ml min^{-1}) for 4 h at 500 °C.

Bimetallic catalysts: they were prepared by the same way as the monometallic ones, but replacing the alumina support by a monometallic catalyst. After impregnation they were also dried, calcined and reduced in the same conditions used for the preparation of monometallic catalysts.

Trimetallic catalysts: they were prepared by the same way as the monometallic catalysts, replacing the alumina support by a bimetallic catalyst and including once more drying, calcination and reduction steps. As all catalysts were prepared with the same support, they are named according to the components of the metallic function (Pt, Pt–Re, Pt–Re–Ge, etc.), where the order for writing the elements is the order of adding the precursors during the catalyst preparation.

The chloride content of the catalysts was determined by the Volhard–Charpenter method. The values were between 0.88 and 1.0% for all of them, an expected value for naphtha reforming catalysts due to the capacity of the support for retaining chloride.

2.2. Catalysts characterization

Temperature programmed reduction: TPR tests were performed in a Micromeritics TPD/TPR 2900 equipment with a thermal conductivity detector. At the beginning of each experiment, the sample was pretreated in situ by heating in air at 450 °C, for 1 h. Then it was heated from room temperature up to 700 °C at 10 °C min^{-1} in a gas stream of 5.0% hydrogen in argon. The average deviation of the measurements was found to be of 4.1%.

CO-FTIR spectroscopy: FTIR spectra in the 4800–400 cm^{-1} range were taken at room temperature in a Perkin Elmer Spectrum One equipment with a resolution of 4 cm^{-1}. Self supported wafers of the catalysts were first reduced at 500 °C under hydrogen flow for 30 min, outgassed at 10^{-6} Torr at 500 °C, for 30 min and then the first spectrum (I) was recorded. After this stage, the samples were kept under 50 Torr of carbon monoxide for 5 min and then a second spectrum (II) was recorded. The adsorption band related to the chemisorbed carbon monoxide was obtained after subtracting the spectra (II − I).

Transmission electron microscopy: TEM were obtained in a JEOL JEM 1200 EXII microscope. The supported catalysts were ground in an agate mortar and dispersed in ethanol. A diluted drop of each dispersion was placed on a 150 mesh copper grid coated with carbon. The micrographs were obtained in both bright and dark fields. A gold strip (Merck 99% pure) was used as standard for calibration.

Temperature programmed desorption of pyridine: the amount and strength of the acid sites of the catalysts were assessed by means of TPD of pyridine. 200 mg of the catalyst were first introduced in a closed vial containing pure pyridine (Merck, 99.9%) for 4 h. Then, the vial was opened and the excess of pyridine was allowed to evaporate at room conditions until the surface of the particles was dried. The sample was then loaded into a quartz tube microreactor and supported over a quartz wool plug. A constant flow of nitrogen (40 ml min^{-1}) was passed over the sample during the experiment. A first step of desorption of weakly adsorbed pyridine and stabilization was performed by heating the sample at 110 °C, for 1 h. Then the temperature of the oven was raised to a final value of 500 °C at

a heating rate of $10\,°C\,min^{-1}$. The reactor outlet was directly connected to a flame ionization detector. The detector signal (in mV) was sampled at 1 Hz and recorded in a computer. The error associated to the peak position and areas has been determined as around 7%.

Cyclohexane dehydrogenation: the evaluation of the catalysts in cyclohexane dehydrogenation was carried out using 100 mg of the sample. A stream of hydrogen was first passed through a cyclohexane saturator. The resulting mixture, with a hydrogen/cyclohexane molar ratio of 18, was fed to the reactor and flowed over the sample. The reactor operated at $400\,°C$ and 1 atm. Before reaction, the catalysts were heated under hydrogen flow ($80\,cm^3\,min^{-1}$) at $500\,°C$, for 1 h. The products were analyzed in a Varian 3400 CX chromatograph equipped with a FID and a packed column of FFAP on Chromosorb. The average error of the measurements was less than 3%.

n-Octane reforming reaction: the activity and selectivity of the catalysts were evaluated in n-octane reforming at $450\,°C$ and atmospheric pressure, for 6 h. n-Octane was used as a model feedstock of a naphtha cut because this is indeed an ubiquitous compound in industrial processes aimed at obtaining BTX cuts (benzene, toluene, xylene). The reactor, containing 0.360 g catalyst, was fed with a hydrogen stream ($38.7\,cm^3\,min^{-1}$) previously saturated in n-octane at $56.7\,°C$. Before the experiments, the samples were heated in nitrogen up to $500\,°C$ and then they were reduced at this temperature with hydrogen for 2 h. The reaction products were analyzed in a VARIAN 3600 CX chromatograph equipped with a flame ionization detector. The average error of the measurements was less than 3%.

Analysis of carbon deposits: the coke deposited on the catalysts during n-octane reforming was analyzed by means of temperature programmed oxidation (TPO). The coked catalyst (30–50 mg) was placed in a quartz cell and the carbon deposits were continuously oxidized with a 6% O_2:N_2 (v/v) stream ($60\,ml\,min^{-1}$). The cell was heated from room temperature up to $650\,°C$ at a heating rate of $10\,°C\,min^{-1}$. The gases issuing from the cell were fed to a methanation reactor where carbon dioxide and carbon monoxide were quantitatively transformed into methane over a nickel catalyst in the presence of hydrogen. The methanator outlet was directly connected to a flame ionization detector and the signal was continuously sampled and recorded. The carbon concentration on the catalysts was calculated from the area under the TPO curves by calibration with TPO tests of standard samples of known carbon content. The average deviation was found to be of 4.1%.

3. Results and discussion

Infrared spectra of the trimetallic samples are displayed in Fig. 1. Carbon monoxide is chemisorbed on platinum particles in linear and bridged forms but is not adsorbed on metallic rhenium or germanium [21]. Fig. 1 shows only the wavenumber region related to linear carbon monoxide, since the band associated to the molecule adsorbed in bridge form, Pt_2CO, is very small and generally not studied. For most spectra, it can be seen an adsorption band with three shoulders, this is related to carbon monoxide linearly adsorbed on platinum sites in different electronic states. The main band, in the $2065–2085\,cm^{-1}$ range, corresponds to the vibrations of carbon monoxide adsorbed on metallic platinum (Pt^0-CO) [23–27]. For all cases, the maximum is shifted to lower wavenumbers in the case of the trimetallic catalysts, as compared to the spectrum of Pt/Al_2O_3 sample, in which this band appears at $2075\,cm^{-1}$, according to previous works [10]. This indicates that platinum is electronically enriched when in contact with the additives. The shoulder observed at higher wavenumbers (around $2120\,cm^{-1}$) can be attributed to platinum under the influence of
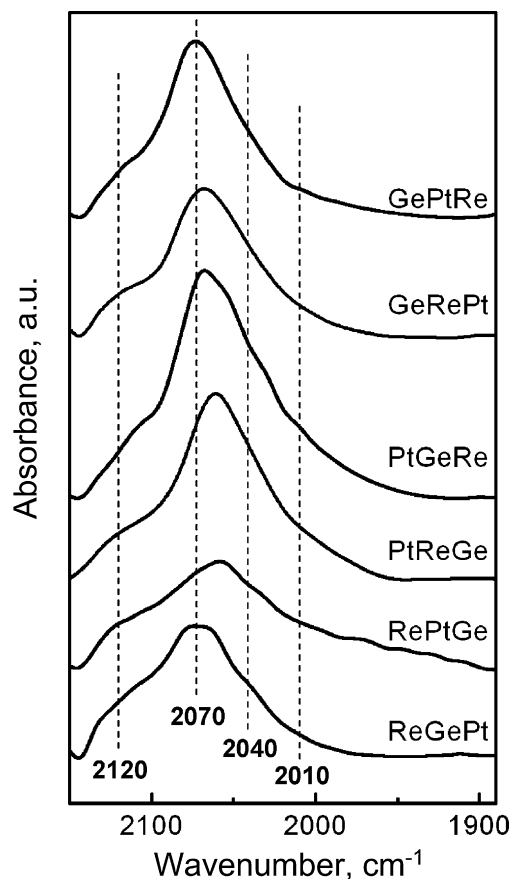
Fig. 1. FTIR spectra of the trimetallic catalysts.

germanium, which acts as an electron acceptor decreasing the electronic density of platinum and making it electron-deficient ($Pt^{\delta+}$) [28]. On the other hand, the shoulder noted around $2010\,cm^{-1}$ can be ascribed to platinum affected by rhenium ($Pt^{\delta-}$-CO); in contrast to the effect caused by germanium, there is an electronic transfer from rhenium to platinum that makes the last one electronically richer [10]. A shoulder at almost $2040\,cm^{-1}$ was also identified, related to platinum species simultaneously interacting with rhenium and germanium.

Once the maximum was shifted to lower frequencies for all trimetallic catalysts, as compared to the platinum monometallic one [10,22], it can be concluded that platinum interacts much more with rhenium than with germanium for all samples. Moreover, when germanium was impregnated after the other metals (PtReGe and RePtGe samples) platinum interacts more strongly with rhenium, as compared to the other samples and the electron-depletion effect of germanium was decreased. As a consequence, the maximum at $2070\,cm^{-1}$ was shifted to lower wavenumbers. On the other hand, the curve of the GePtRe sample shows the smallest decrease in the absorption band at $2070\,cm^{-1}$ (as compared to platinum monometallic catalyst), indicating that platinum is interacting with both rhenium and germanium. The most significant changes in the absorption bands occur for the samples prepared by adding rhenium prior to the other metals (RePtGe and ReGePt samples). In fact, they have the most distorted platinum electron band structure, indicating several electronic states of platinum.

Fig. 2 shows the TPR curves for monometallic and bimetallic catalysts. The curve for Pt/Al_2O_3 catalyst showed a peak at $222\,°C$ due to the reduction of platinum species in weak interaction with the support. A broad peak can be observed at around $388\,°C$ attributed to the reduction of highly dispersed oxychloride species ($PtCl_xO_y$)

Fig. 2. TPR curves of the monometallic and bimetallic catalysts.

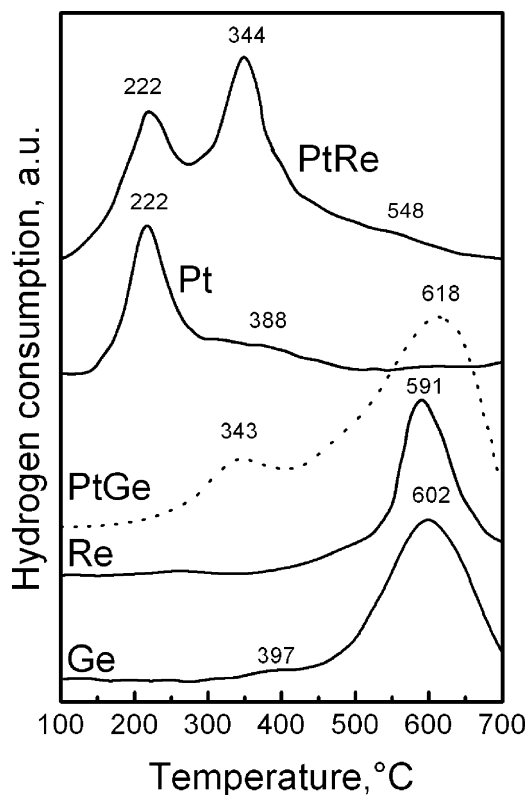**Fig. 3.** TPR curves of the trimetallic catalysts.

in strong interaction with alumina [10,29]. The total hydrogen consumption calculated for the TPR area in Fig. 2 corresponds to the total reduction of Pt(IV) to Pt(0). The TPR curve for rhenium oxide has a peak centered at about 591 °C and a small shoulder at lower temperature (495 °C) that correspond to the reduction of bigger particles in weaker interaction with the support [30]. The hydrogen consumption calculated from the areas under the peaks indicates that about 90% of rhenium oxide is reduced to metallic rhenium. Germanium oxides are reduced at high temperatures, near 600 °C, in agreement with previous results [3].

The curve of PtRe sample shows a low temperature peak at 222 °C, ascribed to the reduction of platinum oxides, weakly interacting with the support. A second peak at 344 °C was also noted, which can be attributed to the reduction of rhenium oxide and to platinum oxide in its neighborhood. The reduction of rhenium oxide occurred at lower temperature, as compared to Re sample, due to the catalytic action of platinum which makes its reduction easier [6,10,31]. The shoulder at 548 °C was associated to the reduction of rhenium oxides in strong interaction with the support, in accordance with previous works [10,22].

The TPR of PtGe sample shows that germanium strongly inhibited the reduction of platinum. This can be easily seen by inspecting the first peak at 343 °C, for the reduction of some isolated platinum species, which was shifted to higher temperatures. The size of the peak at 618 °C that corresponds to segregated germanium species was also increased; this is due to the reduction of the remaining platinum species, in strong interaction with germanium oxide. Previous works on Pt–Ge catalysts reduced at 650 °C [3,5,22] have shown that germanium is present as Ge(II) and Ge(0), the last one alloyed to platinum. The shift of the reduction peaks of platinum oxides to higher temperatures can be attributed to a hindering of the reduction of platinum species by a strong electronic interaction with germanium or to physical blocking [22].
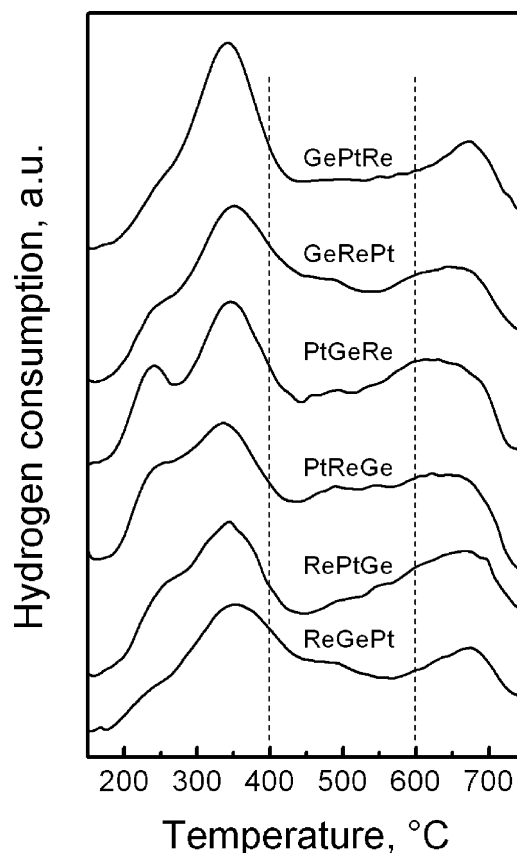
All trimetallic catalysts display many reduction peaks or reduction envelopes, as shown in Fig. 3. There is a first reduction zone from 150 to 400 °C, a second intermediate reduction zone at about 400–600 °C and finally a broad reduction peak at temperatures higher than 600 °C. The first reduction peak at about 240 °C can be attributed to the reduction of oxidized platinum species, while the peak at 340 °C is due to the simultaneous reduction of germanium, rhenium and platinum species. Germanium and rhenium species in strong interaction with platinum were reduced at relatively low temperatures because of the catalytic effect of platinum [6,10,21,22,31]. The intermediate reduction zone (400–600 °C) can be attributed to the reduction of germanium and rhenium species anchored near platinum particles. The high temperature reduction zone (>600 °C) can be associated to the presence of segregated germanium and rhenium species strongly interacting with the support.

The reduction peak of platinum oxidized species at 222 °C on the monometallic platinum catalyst was shifted to higher temperatures (240 °C) on the multimetallic catalysts. The delayed reduction is related to the interaction of platinum with germanium and rhenium, in agreement with the infrared spectroscopy results which have shown interactions among the metals.

Comparing the curves of the trimetallic samples it can be seen that when platinum is impregnated before the other metals (PtGeRe and PtReGe samples) the peak at 250 °C gets sharper, indicating that more segregated platinum particles were produced, as compared to the other samples. On the other hand, when platinum is impregnated after rhenium and/or germanium, the reduction of platinum occurs at higher temperatures. It can also be noted that the peak at 350 °C is narrower for the GePtRe sample than for the other ones, indicating that platinum is more alloyed to the other metals in this solid; besides, just a shoulder is noted around 250 °C while there is no peak in the range of 400–600 °C, suggesting that

Table 1
Hydrogen consumption as a function of reduction zone obtained by TPR for trimetallic catalysts.

Catalysts	Hydrogen consumption ($\mu mol\,g^{-1}$)			
	Total	150–400 °C	400–600 °C	>600 °C
PtReGe	73	34	23	16
PtGeRe	72	37	13	22
RePtGe	55	32	5	18
ReGePt	48	31	6	11
GePtRe	60	35	14	11
GeRePt	71	37	17	17

all platinum was reduced at around 350 °C, together with some rhenium and germanium. This finding is in accordance with the results of infrared spectra, which showed the narrowest peak at 2070 cm^{-1} for this sample, indicating less electronic states of platinum when compared to the other ones. For all cases, a high temperature peak was noted, indicating that some rhenium and/or germanium go into reduction at high temperatures, regardless the order of metal addition. As platinum is interacting much more with rhenium than with germanium, according with FTIR results, this peak is probably more related to germanium, since most of rhenium was expected to be reduced at lower temperature, because of its interaction with platinum.
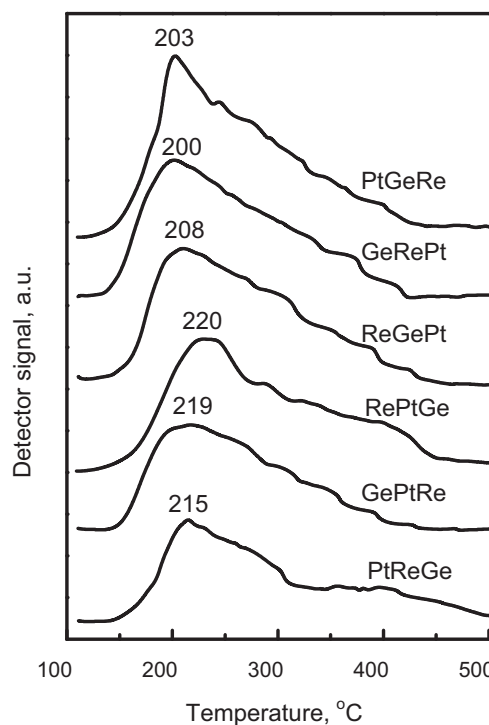
The total hydrogen consumption for all trimetallic catalysts (measured as the total area under the TPR curve) was lower than the sum of the individual values needed for the total reduction of platinum (31 $\mu mol\,g^{-1}$), germanium (83 $\mu mol\,g^{-1}$) and rhenium (56 $\mu mol\,g^{-1}$) monometallic catalysts calculated on the same total metal content basis. This difference confirms that some metal oxide remains unreduced.

According to data in Table 1, which shows the hydrogen consumption during the TPR experiments on trimetallic catalysts, when platinum is impregnated prior to the other metals (PtReGe and PtGeRe samples), the total hydrogen consumption is the highest one among all catalysts and a greater amount of rhenium and germanium is reduced. However, most of these metals are segregated from platinum (the area reduction above 400 °C). A similar behavior was noted for the catalysts prepared by impregnating germanium prior to the other metals but most of the metals are reduced together, as indicated by TPR curves; moreover, less germanium remains unreduced for the GePtRe sample while some platinum species remain segregated for the GeRePt one. The opposite occurred when rhenium was impregnated before the other metals (RePtGe and ReGePt samples). The total hydrogen consumptions were lower and lesser amount of rhenium and germanium oxides, located in the vicinity of platinum (area 400–600 °C), was reduced. In such cases, the hydrogen consumption related to the first reduction area was equivalent to that required to reduce only platinum oxide, indicating that the catalytic effect of platinum on the reduction of other metals was decreased.

Table 2 shows the results of the acidity measurements. The area values under the TPD curve (Fig. 4) are proportional to the total concentration of acid sites, while the maximum peak temperature is a

Fig. 4. TPD curves of the trimetallic catalysts.

parameter that can be used to evaluate the strength of acidic sites. Previous results [12] showed that chlorided alumina support has a main desorption peak of pyridine at 220 °C and that the addition of platinum and rhenium decreases the total amount of pyridine adsorbed. Germanium addition also decreases the acidity of the support [26]. It can be seen in Table 2 that the addition of germanium, platinum and rhenium decreases the temperature of the main pyridine desorption peak, except for the RePtGe and GePtRe catalysts. This means that the addition of the metals does not increase the strength of the sites of higher acidity. It can be noted that there are not meaningful differences among the catalysts, indicating that the order of metal addition does not significantly affect the acidity of the catalysts. These results are not in accordance with those previously found for the PtReSn system, which showed a strong influence of the order of metals addition on the acidity of the catalysts [12]. The difference can be assigned to the fact that platinum and rhenium oxidized species are acidic while tin species are basic and in the case of the PtReGe system all oxidized species are acidic.

The activity of the metal function is clearly affected by the order of metals addition, as shown by the results of conversion of cyclohexane reported in Table 3. Cyclohexane dehydrogenation is an insensitive structure reaction, completely selective to the formation of benzene. Therefore, the activity level of the catalyst in this reaction is proportional to the amount of accessible metal surface sites. Moreover, the dehydrogenation activity is due to surface

Table 2
Area of pyridine and temperature of the main peak in TPD curves.

Catalysts	Pyridine TPD tests	
	Curve area (a.u.)	Temperature of the main peak (°C)
PtReGe	0.76	215
PtGeRe	1.00	203
RePtGe	0.90	220
ReGePt	0.92	208
GePtRe	0.83	219
GeRePt	0.93	200

Table 3
Average size of the metal particles obtained by TEM and cyclohexane conversion on the catalysts.

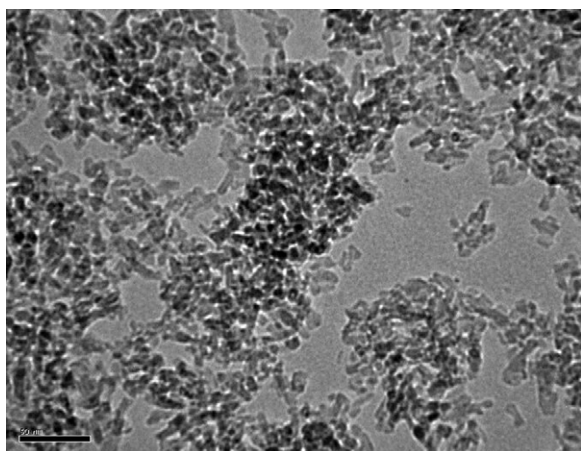| Catalysts	Mean diameter (nm)	Cyclohexane conversion (%)
PtReGe	1.8	9.3
PtGeRe	2.3	8.2
RePtGe	1.6	6.6
ReGePt	1.7	7.8
GePtRe	2.0	6.2
GeRePt	1.5	5.4

Fig. 5. Transmission electron micrograph of the GeRePt/Al$_2$O$_3$ sample.

platinum atoms, rhenium has a very low activity and germanium is not active. For this reason the cyclohexane conversion is only related to platinum superficial atoms. In spite of this, the activity of platinum is influenced by other metals by means of geometrical (blockage) or electronic effects. In a previous work [10], we pointed out that the electronic effect is more important than the geometric one. From Table 3, it can be noted that the samples prepared by impregnating platinum before the other metals (PtReGe and PtGeRe samples) are more active than the others. These results are in agreement with those of TPR experiments, which showed that for these samples platinum is mostly segregated from the other metals; then platinum is almost not affected by the other metals. On the other hand, the catalysts obtained by impregnating germanium prior to platinum and rhenium are the least active ones, since there are stronger interactions among the metals.

It can also be seen from Table 3 that the dehydrogenation activity has no relationship with the particles size. This result can be explained by considering that particles can be formed by different ensembles of platinum, rhenium and germanium atoms, resulting in platinum species with different electronic states. The dehydrogenation activity of platinum can therefore be strongly modified by the interaction with the other metals, as shown by the results. Fig. 5 illustrates a typical image for trimetallic catalysts obtained by TEM.

n-Octane reforming is a very useful tool to evaluate the performance of reforming catalyst because it requires both functions (metal and acid). The reaction mechanism is bifunctional but it is controlled by the acid function where the isomerization and cyclization steps take place. There are also reactions only catalyzed by the metal function, such as hydrogenolysis and dehydrogenation. Some other reactions, such as cracking, proceed by an acid monofunctional mechanism. Fig. 6 shows the values of the initial (5 min time-on-stream) n-octane conversion and the carbon deposited on the catalysts as a function of the deactivation degree (X). This is defined as $X = (X_{min} - X_{360\,min})/(X_{5\,min})$) and is a measurement of the relative deactivation during reaction. In general, the conversion of n-C$_8$ does not depend on the order of addition of metal precursors, except for GeRePt and RePtGe samples. The GeRePt catalyst shows the highest activity while the RePtGe sample shows the lowest one.

It can be seen also in Fig. 6 that the coke deposited on the catalysts (carbon content) increases with n-octane conversion, indicating that the catalysts deactivation is due to carbon deposited on both metal and acid sites. This is confirmed by the TPO curves (Fig. 7) in which one can see a low temperature peak (150–180 °C) assigned to the burning of a small amount of coke deposited on metallic sites. As pointed out previously by several workers
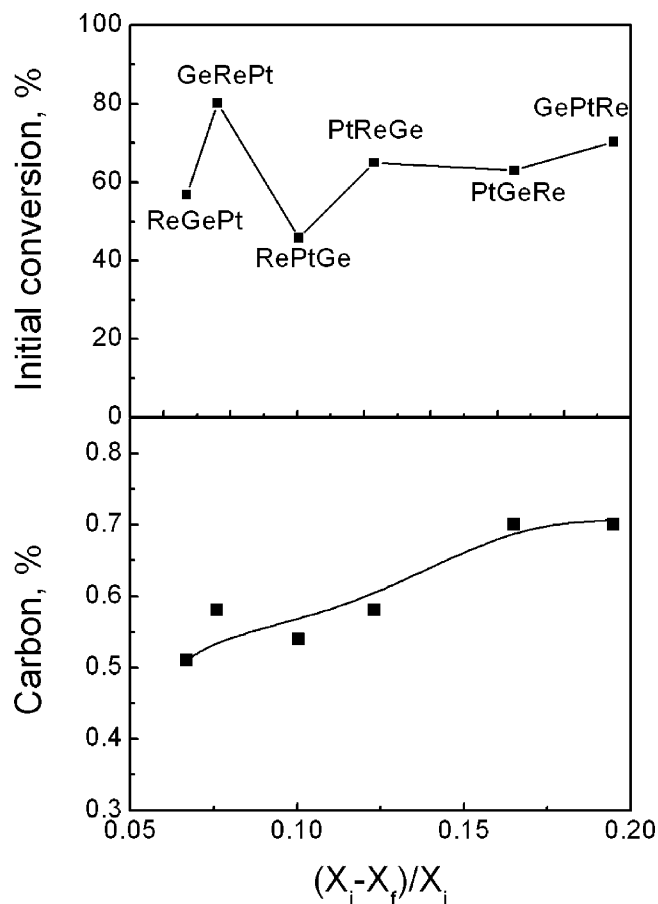

Fig. 6. n-Octane reforming reaction. Initial conversion and amount of deposited carbon as a function of the degree of deactivation.
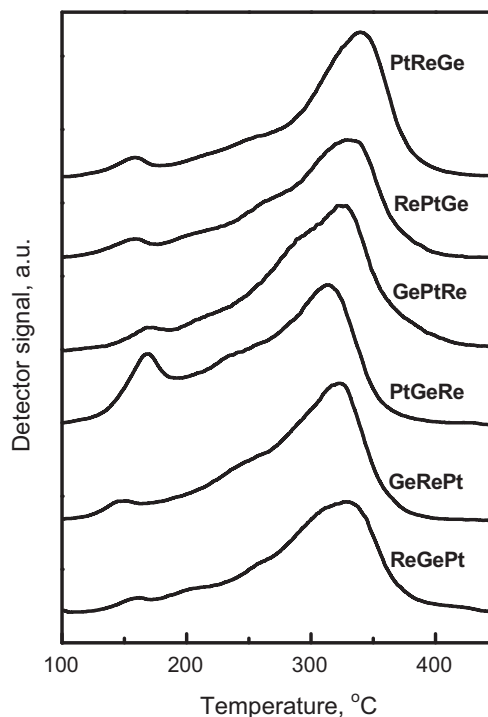

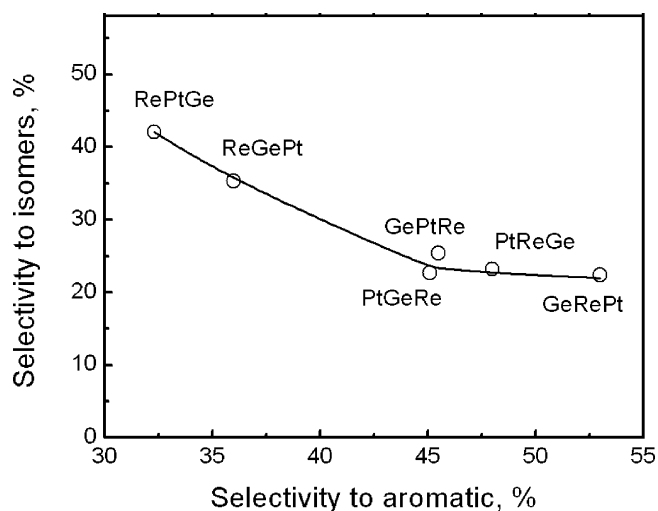**Fig. 7.** TPO profiles of the trimetallic catalysts.

Fig. 8. n-Octane reforming reaction. Selectivity to isoparaffins as a function of selectivity to aromatics content after 360 min time-on-stream.

[12,16,32,33], this coke is poorly polymerized and rich in hydrogen, being easy to burn. The high temperature peak, located at about 330 °C, corresponds to the burning of coke deposited on alumina, which is more polymerized and poor in hydrogen and thus difficult to burn [12,16,32,33]. There is also an intermediate zone of coke burning, related to coke deposits of intermediate degree of polymerization and to deposits located in the vicinity of platinum [12]. It can be noted that, in the reaction conditions used in this work (atmospheric pressure), coking is important and a great decrease of the catalytic activity occurs in a short reaction time. The GePtRe sample had the lowest stability, as shown by the plots of the deactivation parameter and final coke content. Conversely, the ReGePt catalyst was the most stable one.

Fig. 8 shows the values of the isomers selectivity as a function of the aromatics selectivity. It can be seen that the selectivity to isomers decreases as the selectivity to aromatics increases. It is interesting to see that while the total activity (level of conversion of n-C$_8$) varies only slightly with the order of addition of the metal salts, the selectivity to isoparaffins or aromatics is drastically changed. However, the sum of the selectivities to isoparaffins and aromatics remains practically constant whichever the order of addition used. The accepted kinetic mechanism for the formation of aromatics or isoparaffins is bifunctional. Olefins are first produced on metal sites and then they are isomerized or transformed over the acid sites [1]. The reactions on the acid sites are the slowest ones and therefore they are rate-controlling. The data of Fig. 8 indicate that when the interaction among platinum and rhenium is high (PtReGe, PtGeRe) the rate of formation of aromatics is higher than the rate of formation of isoparaffins. This is an evidence that germanium and rhenium oxides in the vicinity of platinum modify the acidity of the support and favor dehydrocyclization.

Fig. 9 shows values of selectivity to methane obtained at the end of n-C$_8$ reforming as a function of cyclohexane conversion. It can be seen that as the dehydrogenation capacity is higher, the hydrogenolytic activity is lower. As mentioned earlier, cyclohexane dehydrogenation is a non-demanding reaction and hence should only depend on the amount of available platinum surface sites. In contrast, hydrogenolysis is a demanding reaction that needs an ensemble of adjacent metal atoms in order to take place. The hydrogenolytic activity can be taken as an indirect measure of the Pt–Re interaction [34] because of the synergetic effect between the metals. This effect has been explained by considering the adsorption heat of hydrocarbons over platinum and rhenium. Hydrocarbons are strongly adsorbed on rhenium and very weakly
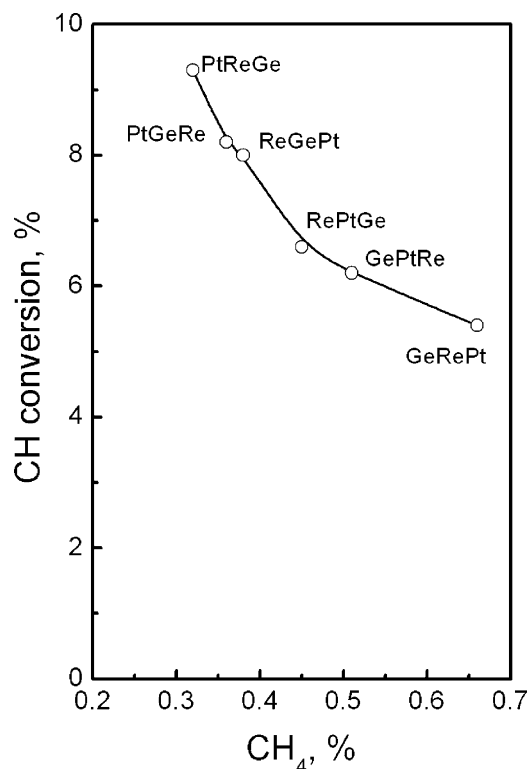

Fig. 9. Cyclohexane conversion as a function of selectivity to methane in n-octane reforming reaction after 360 min time-on-stream.

on platinum and then the desorption of products is the limiting factor in the first case and the adsorption of reactants in the last one. Therefore, an intermediate composition exists for which the reaction rate is maximum [2,34]. The synergy of the metals has also been explained in terms of different ensemble structures [35]. Previous results [36] indicate that the higher the Pt–Re interaction the higher the hydrogenolytic activity and the lower the dehydrogenating one. This can be related to the fact that the dehydrogenating activity is due to the presence of only platinum atoms while the hydrogenolytic activity is mainly due to Pt–Re ensembles, separate platinum and rhenium atoms are less active in hydrogenolysis than these ensembles. The addition of germanium inhibits both hydrogenolytic and dehydrogenating functions [22]. Therefore, the phenomenon of high Pt–Re interaction and its relationship with high hydrogenolysis and low dehydrogenation capacity is also present in trimetallic catalysts. As shown by FTIR-CO, platinum is interacting more strongly with rhenium than with germanium. Even though, this effect should occur in a lower extent due to the passivating effect of germanium. As shown by FTIR-CO and TPR, some germanium interacts with platinum for all catalysts. From Fig. 9, it can be noted that the catalysts prepared by impregnating platinum before the other metals are the least active to hydrogenolysis, this is due to the low interaction among the metals, as shown by TPR and FTIR-CO. The opposite happens for the catalysts obtained by the impregnation of germanium before platinum and rhenium, which showed the highest activity due to the stronger interaction among the metals. When rhenium is impregnated before the other metals, catalysts with intermediate behavior were obtained.

4. Conclusions

The order of addition of the metal precursors during the preparation of Pt–Re–Ge/Al$_2$O$_3$ catalysts largely affects the

properties and the catalytic performance of these systems in n-octane reforming. The impregnation of platinum prior to rhenium and germanium decreases the interaction among the metals whose majority is reduced independently, producing catalysts highly active in cyclohexane dehydrogenation and less active in n-octane hydrogenolysis. On the other hand, by impregnating germanium prior to the other metals, catalysts with low activity in dehydrogenation and high activity in hydrogenolysis are obtained, as a consequence of the strong interactions among the metals. By adding rhenium before the other metals, catalysts with intermediate behavior are produced. For all catalysts, the electronic properties of platinum were more affected by rhenium as compared to germanium. The order of addition of the metal precursors does not modify the acidic properties of the support but germanium and rhenium seem to change the acidity of the support in the vicinity of the metals, causing differences in the selectivities to aromatic compounds and paraffinic isomers. Therefore, depending on the purpose of the reforming process, i.e. the production of aromatics or the production of isoparaffins-rich gasoline, the catalyst properties can be tailored by choosing a different order of addition of the metal precursors. The RePtGe catalysts have a higher selectivity to branched isoparaffins while a reformate rich in aromatics can be obtained over the GeRePt catalyst.

Acknowledgments

References

[1] J.M. Parera, N.S. Fígoli, in: G.J. Antos, A.M. Aitani, J.M. Parera (Eds.), Catalytic Naphtha Reforming: Science and Technology, Marcel Dekker Inc, New York, 1995, pp. 45–78.
[2] S.M. Augustine, W.M.H. Sachtler, J. Phys. Chem. 91 (1987) 5953–5956.
[3] S.R. de Miguel, O.A. Scelza, A.A. Castro, Appl. Catal. A: Gen. 44 (1988) 23–32.
[4] L.S. Carvalho, P. Reyes, G. Pecchi, N.S. Fígoli, C.L. Pieck, M.C. Rangel, Ind. Eng. Chem. Res. 40 (2001) 5557–5563.
[5] S.R. de Miguel, J.A. Martinez Correa, G.T. Baronetti, A.A. Castro, O.A. Scelza, Appl. Catal. A: Gen. 60 (1990) 47–59.
[6] L.Y. Chen, Y.Q. Ni, J.L. Zang, L.W. Lin, X.H. Luo, S. Cheng, J. Catal. 145 (1994) 132–140.
[7] M.C. Rangel, L.S. Carvalho, P. Reyes, J.M. Parera, N.S. Fígoli, Catal. Lett. 64 (2000) 171–178.
[8] F.M. Dautzenberg, J.N. Helle, P. Biloen, W.M.H. Sachtler, J. Catal. 63 (1980) 119–128.
[9] C. Kappesnstein, M. Saouabe, M. Guérin, P. Marecot, I. Uszkurat, Z. Paál, Catal. Lett. 31 (1995) 9–17.
[10] L.S. Carvalho, C.L. Pieck, M.C. Rangel, N.S. Fígoli, J.M. Grau, P. Reyes, J.M. Parera, Appl. Catal. A: Gen. 269 (2004) 91–103.
[11] F. Epron, C. Carnevillier, P. Marécot, Appl. Catal. A: Gen. 295 (2005) 157–169.
[12] L.S. Carvalho, C.L. Pieck, M.C. Rangel, N.S. Fígoli, C.R. Vera, J.M. Parera, Appl. Catal. A: Gen. 269 (2004) 105–116.
[13] C.L. Pieck, C.R. Vera, J.M. Parera, G.N. Giménez, L.R. Serra, L.S. Carvalho, M.C. Rangel, Catal. Today 107–108 (2005) 637–642.
[14] A. Jahel, P. Avenier, S. Lacombe, J. Olivier-Fourcade, J.-C. Jumas, J. Catal. 272 (2010) 275–286.
[15] V.M. Benitez, C.R. Vera, M.C. Rangel, J.C. Yori, J.M. Grau, C.L. Pieck, Ind. Eng. Chem. Res. 48 (2009) 671–676.
[16] L.S. Carvalho, C.L. Pieck, M.C. Rangel, N.S. Fígoli, J.M. Parera, Ind. Eng. Chem. Res. 43 (2004) 1222–1226.
[17] K.R. McCallister, T.P. O'Neal, French Patent 2,078,056, to UOP (1971).
[18] R.E. Rausch, U.S. Patent 3,745,112, to UOP (1975).
[19] J.H. Sinfelt, U.S. Patent 3,953,368, to Exxon (1976).
[20] L.I. Ali, A.G. Ali, S.M. Aboul-Fotouh, A.K. Aboul-Gheit, Appl. Catal. A: Gen. 205 (2001) 129–146.
[21] V.A. Mazzieri, C.L. Pieck, C.R. Vera, J.C. Yori, J.M. Grau, Appl. Catal. A: Gen. 353 (2009) 93–100.
[22] M.C.S. Santos, J.M. Grau, C.L. Pieck, J.M. Parera, J.L.G. Fierro, N.S. Fígoli, M.C. Rangel, Catal. Lett. 103 (2005) 229–237.
[23] P. Hollins, Surf. Sci. Rep. 16 (1992) 51–94.
[24] J.A. Anderson, C.H. Rochester, Catal. Today 10 (1991) 275–282.
[25] F. Boccuzzi, G. Ghiotti, A. Chiorino, L. Marchese, Surf. Sci. 233 (1990) 141–152.
[26] J.A. Anderson, M.G.V. Mordente, C.H. Rochester, J. Chem. Soc. Faraday Trans. I 85 (1989) 2983–2990.
[27] M.G.V. Mordente, C.H. Rochester, J. Chem. Soc. Faraday Trans. I 85 (1989) 3495–3504.
[28] N. Macleod, J.R. Fryer, D. Stirling, G. Webb, Catal. Today 46 (1998) 37–54.
[29] H. Lieske, G. Lietz, H. Spindler, J. Volter, J. Catal. 81 (1983) 8–16.
[30] R.L. Meiville, J. Catal. 87 (1984) 437–442.
[31] B.H. Isaac, E.E. Petersen, J. Catal. 85 (1984) 8–15.
[32] M.C. Rangel, M.N.M. Barbosa, C.L. Pieck, N.S. Fígoli, Stud. Surf. Sci. Catal. 111 (1997) 415–420.
[33] P. Marécot, J. Barbier, in: G.J. Antos, A.M. Aitani, J.M. Parera (Eds.), Catalytic Naphtha Reforming: Science and Technology, Marcel Dekker Inc, New York, 1995, pp. 279–311.
[34] S.M. Augustine, W.M.H. Sachtler, J. Catal. 106 (1987) 417–427.
[35] C. Betizeau, G. Leclercq, R. Maurel, C. Bolivar, H. Charcosset, R. Frety, L. Toumayan, J. Catal. 45 (1976) 179–188.
[36] C.L. Pieck, P. Marécot, J.M. Parera, J. Barbier, Appl. Catal. A: Gen. 126 (1995) 153–163.